Measurement of the electrical resistivity of cement-based materials using post-embedded probes: effect of contact material

Authors:

M. Messina [1], A. Belda Revert [2,3], M. Gastaldi [4], M.R. Geiker [5]

[1]PhD student, Politecnico di Milano, Department of Chemistry, Materials and Chemical Engineering "G. Natta", Via Mancinelli 7, 20131 Milan, Italy. email: marco.messina@polimi.it

[2]PhD student, Norwegian University of Science and Technology, Department of Structural Engineering, Richard Birkelands vei 1a, NO-7491 Trondheim, Norway.

[3]OPAK AS, Engebrets vei 7, 0275 Oslo. email: abr@opak.no

[4]Associate professor, Politecnico di Milano, Department of Chemistry, Materials and Chemical Engineering "G. Natta" Via Mancinelli 7, 20131 Milan, Italy. email: matteo.gastaldi@polimi.it

[5]Professor, Norwegian University of Science and Technology, Department of Structural Engineering, Richard Birkelands vei 1a, NO-7491 Trondheim, Norway. email: mette.geiker@ntnu.no

Keywords: cement-based material; mortar; electrical resistivity; grout; post-embedded probe; numerical simulations.

ABSTRACT

The measurement of the electrical resistivity of cement-based materials, e.g., concrete, is used for quality control and durability assessment. In an existing structure, the electrical resistivity of the concrete can be monitored using either pre- or post-embedded probes. When using post-embedded probes, the contact material (grout) used when installing the probe can affect the measurements. This work investigated the effect on the measurement of two different grouts (in alkaline and carbonated condition) used for the installation of a post-embedded probe in carbonated mortar. The effect of the geometry of the system was also examined.

1. INTRODUCTION

The electrical resistivity is one of the key parameters in the durability assessment of reinforced concrete structures. Electrical resistivity data is e.g., used for quality control of material consistency and presence of supplementary cementitious materials and to evaluate the resistance to chloride penetration [3-5], or the potential steel reinforcement corrosion rate [6-10], concrete moisture condition [1-2] and the susceptibility to other damage mechanisms as freeze/thaw and alkalis silica reactions, and it was suggested as input data for service life prediction of reinforced concrete structures [11-12].

The electrical resistivity represents the material's ability to withstand the flow of electrical current and can give useful information about the changes of the characteristics of the material. The electrical resistivity of concrete after casting is usually very low (in the order of few tens of Ω·m), while hardened concrete can vary over a wide range: from a few tens of Ω·m in saturated condition to many thousands of Ω·m in dry conditions [13]. In addition to the degree of saturation, the electrical resistivity depends on the microstructure of the material, the composition of the pore solution, and the temperature. A reduction of the water-to-cement ratio, an increase of the time of curing, or the use of blended cements instead of Portland cement cause an increase in the electrical resistivity (at fixed degree of saturation) [14]. The electrical resistivity increases when the ion concentration in the pore solution is reduced [15]. This can occur, for example, when concrete is subjected to carbonation. In this process, the carbon dioxide significantly reduces the concentration of hydroxide ions, but also the concentration of other ions is affected [16]. The temperature, among others, affects the ion mobility and the water vapour sorption isotherm [17]. In general, the electrical resistivity increases with reduced temperature and vice versa [18].

The resistivity of concrete can be measured by means of different techniques following general recommendations based on past research experiences [19]. In the context of field assessment of reinforced concrete structures, the electrical resistivity is usually measured using a surface-applied two or four electrodes probe (Figure 1a) [20]. This technique primarily measures the condition of the concrete cover. However, the concrete cover may not be representative for the condition at the

steel-concrete interface. The discrepancy is mainly explained by the wall effect affecting both the cover and the steel-concrete interface (but at different scales), curing affecting the microstructure of the outer part of the cover [21], and the exposure affecting the moisture distribution. Continuous wetting and drying causes the convection zone to become more conductive during rainfall and less conductive during sun and wind exposure. Moreover, the external probe cannot be used on a concrete surface treated with insulating coating [22] and practical limitations are faced to perform long-term field monitoring. An alternative could be the use of post-embedded probes placed at the same depth as the reinforcement (Figure 1b). A contact material is required between concrete and post-embedded probes when using post-embedded probes. Few works have investigated the application of post-embedded probes [23-24] and the effect of contact material on the concrete electrical resistivity was not studied.

Therefore, the aim of this work was to examine the effect of the contact material used when post-embedding a two-wire electrical resistivity probe in carbonated mortar. Both alkaline and carbonated cement grout were used as contact material. Experimental data obtained with this probe type and traditional external plates were compared, and the impact of the grout and the geometry of the system was assessed using numerical simulations. AC was used to avoid polarization at the electrodes.

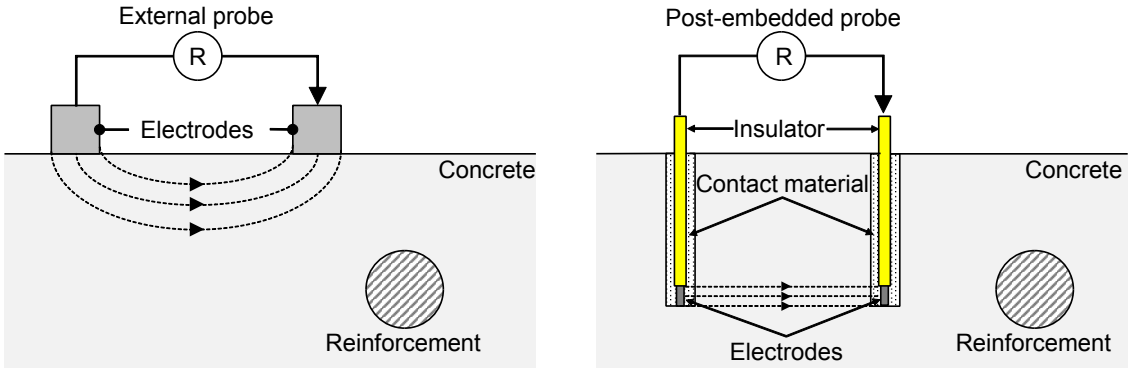

(a) (b)

Figure 1. Schematic representation of electrical resistivity measurement on a reinforced concrete structure: (a) external probe placed on the concrete surface; (b) post-embedded probe placed at the same depth as the reinforcement. The sketches show how current flows between the emitter and receiver electrodes. The direction would be constant (as shown here) for DC measurements but is continuously switching for AC as used in this study.

2 MATERIALS AND METHODS

2.1 Experimental tests

Carbonated mortar prisms were used to investigate the influence of the contact material on the measurement of electrical resistivity using post-embedded probes. Grout was used as contact material. Cylindrical grout specimens were prepared to investigate the effect of the electrode position (embedded or external) on the measurement of the electrical resistivity and determine the electrical resistivity of the grout. Table 1 presents an overview of the specimens.

The mortar prisms (160 mm x 40 mm x 40 mm) were cast and cured, and fully carbonated. Carbonation was assessed by spraying a thymolphthalein solution on freshly split surface. After carbonation, one two-wire electrode probe was post-installed in each prism for measurement of the electrical resistivity. At the end of the tests, two cubes (40 mm x 40 mm x 40 mm) were cut from the two ends of each prism (four cubes in total) to measure the resistivity of the mortar.

To investigate the effect of the contact material on the measurement of electrical resistivity of the mortar, two different grouts were used: a commercial Portland cement-based grout and a custom-made portland-fly ash cement-based grout. Each was studied in both alkaline and carbonated condition.

The resistivity measurements were performed on specimens in capillary saturated condition (constant mass after immersion in water bath). The first series of resistivity measurements with the post embedded probes were performed when the grout was alkaline, while the second series of resistivity measurements were performed after the grout had carbonated. Note that data from specimens obtained after carbonation of the grout are labelled with a suffix “-C”.

Table 1. Description of the specimens used in the tests (M: carbonated mortar, postEm: post-embedded probe, Em: probe embedded before casting, Ex: external probe; Ø: diameter, h: height. The designation is for the specimens with alkaline contact material (grout). Data from specimens obtained after carbonation of the grout are labelled with a suffix “-C”.

Designation	Quanti	Material	Dimension (mm)	Probe	Schematic representation
M-postEm-GFA	1	Mortar (MFA)	160x40x40	Post-embedded using grout GFA	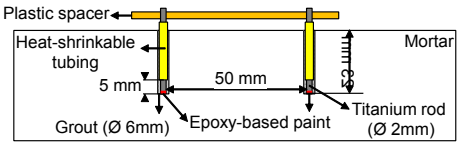
M-postEm-GPM	1	Mortar (MFA)	160x40x40	Post-embedded using grout GPM	
GFA-Em	2	Grout (GFA)	31.5(Ø)x60(h)	Embedded before casting	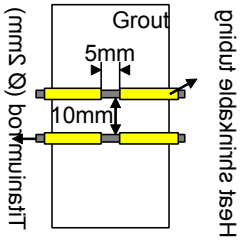
GPM-Em	2	Grout (GPM)	31.5(Ø)x60(h)	Embedded before casting	
GPM-Ex	1	Grout (GPM)	31.5(Ø)x40(h)	External	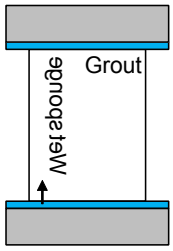
M-Ex	4	Mortar (MFA)	40x40x40	External	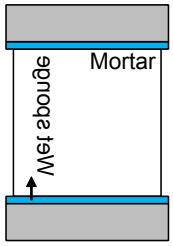

Mortar prisms with post-embedded probes and mortar cubes

The mortar prisms were prepared using 450 g of portland-fly ash cement (CEM II/B-V with 30% of fly ash), 247.5 g of tap water (water to cement ratio of 0.55) and 1350 g of sand. The prisms were cast in standard steel moulds (40x40x160 mm), cured for 14 days at 20°C and relative humidity (RH) higher than 95%, and subsequently exposed to 20°C, 60% RH and 1.5% of CO_2 until they were fully carbonated (> 100 weeks). The carbonation assessment was performed by spraying a 1 % thymolphtalein solution on a freshly split surface in parallel specimens.

A two-wire electrode probe was post-embedded in each prism for measuring the electrical resistivity. For the installation of the probe two holes of 6 mm in diameter and 23 mm in depth were drilled at 50 mm from each (Table 1). The holes were first cleaned by compressed air, the samples were submerged in water for some minutes, superficially dried (also in the holes), and then a cement grout was injected in the holes and the probe was placed in position. Two different types of cement grout were used, see below. After the post-installation of the probe, the prisms were stored for seven days at RH higher than 95%.

Grouts and grout specimens

Two types of cement grout were used as contact material for the post-embedded probes and preparing cylinders for determination of their electrical resistivity.

One grout (GFA) was prepared from portland-fly ash cement (CEM II/B-V with 30% of fly ash), tap water and sieved sand (maximum diameter of 250 μm) in a ratio 1:0.45:1. The other grout (GPM) was prepared from a pre-mixed commercial product (Nonset 50 from Mapei S.p.A). According to the safety data sheet, the material contains Portland cement (approximately 75%), filler and admixture. The GPM was mixed from Nonset 50 and tap water in a ratio 3:1.08 as prescribed in the technical data sheet.

Two cylindrical samples (Ø: 31.5 mm; h: 60 mm) with (pre-)embedded probes were cast from each grout, an additional smaller cylinder (Ø: 31.5 mm; h: 40 mm) without a probe was cast from GPM (Table 1). The smaller cylinder was used for the external measurement of the electrical resistivity. All cylindrical samples were cured for seven days in sealed plastic.

Resistivity probes

The two wire electrodes were made of titanium (2 mm in diameter) and only the outer 5 mm of the wire were not electrically insulated by heat-shrinkable tubing.

Exposure

After the seven days of curing of the grout, all the samples were submerged in tap water until constant mass (mass change lower than 0.01%/24 h), which was obtained after approximately two weeks. The mass of the samples was measured with a balance of accuracy 0.005 g. (The

electrical resistivity was measured after constant mass was achieved (state: carbonated mortar and alkaline grout).

Afterwards, the specimens were dried in a ventilated oven at 28°C for about four weeks and then subjected to accelerated carbonation (20°C, 60% R.H. and 100% of CO_2) for about eight weeks to carbonate the grouts, Subsequently, they were submerged again in tap water until constant mass (approximately two weeks). Electrical resistivity was again measured after constant mass was achieved (state: carbonated mortar and carbonated grout).

Methods

The electrical resistivity was measured with a portable conductivity meter (model HD2156.2 of DeltaOHM). This instrument applies a sinusoidal signal to avoid polarisation of the electrodes. The electrical conductivity was converted into the electrical resistivity (ρ) by means of the cell constant, which were experimentally determined for the embedded probes using solutions of different conductivities.

The external electrical resistivity measurements were carried out using two stainless steel plates (50 mm x 50 mm x 5 mm) as electrodes which were applied on the opposite side of the sample and interposing a wet sponge (Table 1).

2.2 Numerical simulations

Numerical simulations were performed to predict the electrical resistivity of the mortar when using the post-embedded probe in the same configuration used in the experimental tests (Figure 2). The Comsol Multiphysics 5.0 software was applied, and a tetrahedral mesh of varying size was adopted to have higher resolution in the vicinity of the two electrodes and a lower resolution in the bulk. As general boundary conditions, Ohm's law (1) with the continuity equation (2) were applied:

$$-\nabla\varphi = \rho\vec{J} \tag{1}$$

$$\nabla\vec{J} = 0 \tag{2}$$

where φ is the electrical potential, ρ is the electrical resistivity and $\vec{J}$ is the electrical current density vector. The potential difference between the emitter electrode and the receiver electrode was fixed equal to 1V in all the simulations and the electrical current density was obtained from the FE analysis. The electrical current density was used to calculate the electrical resistance between the two electrodes by Ohm's law and subsequently converted into the electrical resistivity by the cell constant.

The system made by the post-embedded probe, the grout and the mortar can be represented by means of a simplified electrical circuit in which each material is associated to an electrical resistance.
A schematic representation of the simplified equivalent electrical circuit is illustrated in Figure 3. The electrical current, circulating between the two electrodes, must pass through the grout, mortar and grout that are in series. According to equation (3), the measured resistance will be the sum of each resistance:

$$R_{system} = R_{grout1} + R_{mortar} + R_{grout2} \quad (3)$$

where R_{grout1} and R_{grout2} are the resistances (Ω) of the grout used as contact material in the two holes, R_{mortar} is the resistance (Ω) of the carbonated mortar, and R_{system} is the resistance of the system, sum of all the resistances. Assuming $R_{grout1} = R_{grout2}$ and using the second Ohm's law, each resistance is given by the electrical resistivity of the material and the cell constant, as shown in the equation (4):

$$\rho_{system}*k_{system} = 2*\rho_{grout}*k_{grout} + \rho_{mortar}*k_{mortar} \quad (4)$$

where the ρ_{grout} is the resistivity (Ω·m) of the grout in the two holes; ρ_{mortar} is the resistivity (Ω·m) of the mortar, ρ_{system} is the weighted sum of all the resistivities (Ω·m), and k_{system} is the cell constant of the system.

Equation (4) suggests that the measurement of electrical resistivity with the post-embedded probe will be a weighted sum of the resistivity of the grout and that of the carbonated mortar. The weights are the cell constants. By knowing the cell constants, it is possible to determine the mortar resistivity from the measurement achieved by the post-embedded probe.

As an example, the results of an iteration procedure are reported in Figure 4. The electrical resistivity of the grout in alkaline condition (specimen GFA-Em) measured experimentally was used as input data and the electrical resistivity of mortar was determined by inverse analysis to fit the electrical resistivity measured with the post-embedded probe (specimen M-postEM-GFA). The discrepancy between the schematic current flow between the tips of the electrodes in Figure 1 and the current flow distribution in Figure 4 is explained by the high conductivity of the alkaline grout which was used for this simulation.

The finite element model was also used for a parametric study of the effect of selected parameters on the electrical resistivity measured with the post-embedded probe: the grout and mortar resistivity, the thickness of the grout, and the electrode distance.

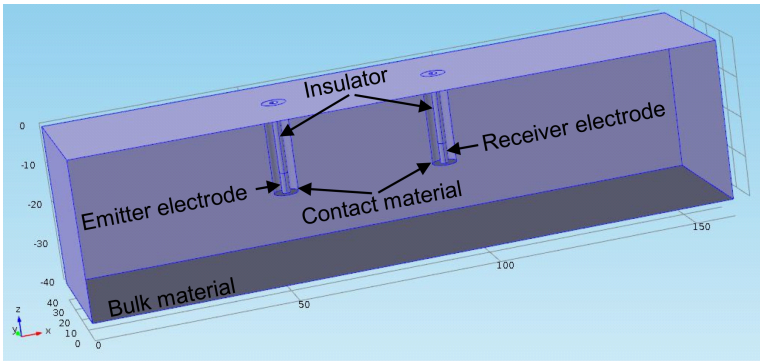

Figure 2. Geometry used in the numerical simulation (160 mm x 40 mm x 40 mm).

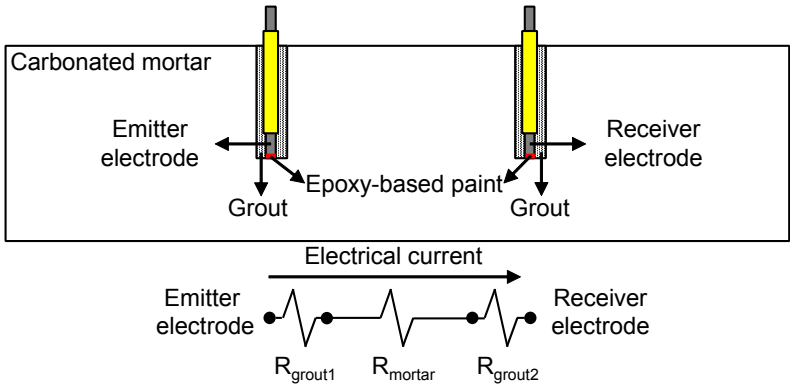

Figure 3. Simplified equivalent electric circuit between the emitter electrode and the receiver electrode when using the post-embedded probe. (AC was used, i.e., the emitter and receiver electrodes were continuously switching place).

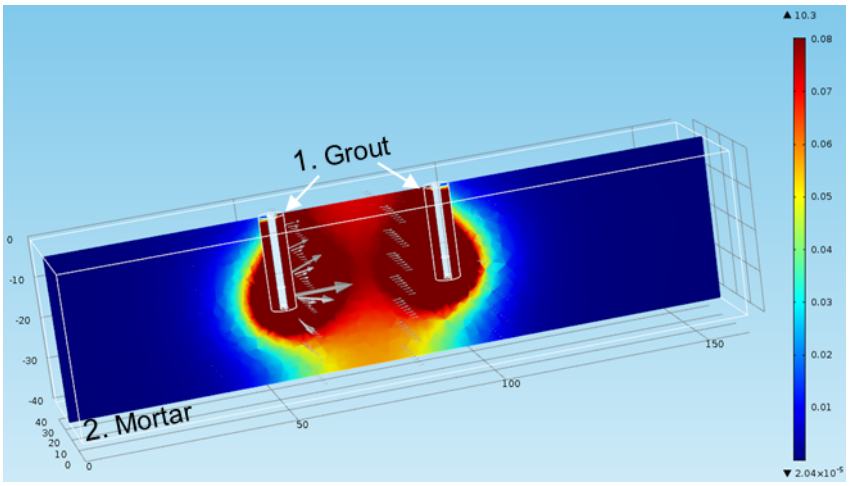

Figure 4. Example of result from FEM simulation of current flow between the emitter electrode and the receiver electrode when using the post-embedded probe in a mortar bar. This example is for carbonated mortar and alkaline grout. Note when using AC emitter and receiver electrodes are continuously switching. The colour indicates the value of the current density.

3 RESULTS AND DISCUSSION

3.1 Comparison of pre-embedded and external probes

These tests were performed on commercial grout (GPM) in saturated condition. The comparison between the measurements of electrical resistivity carried out by means of the pre-embedded probe (specimen GPM-Em) and with the external probe (specimen GPM- Ex) commonly used to measure the electrical resistivity of concrete samples [19], is reported in Figure 5. The mean value of the grout resistivity determined with the two methods was of about 21 Ω·m with pre-embedded probe and 24 Ω·m with the external plates. McCarter and co-workers [25] also compared electrical resistivity measurements using pre-embedded and external probes and observed a slightly higher electrical resistivity when using external probes, a difference which became almost negligible when increasing the electrical resistivity of sample. McCarter and co-workers [25] ascribed the measured increased resistivity to two wet sponges introducing two additional very small resistances in series to the simplified equivalent electrical circuit that can be used to describe the system (see Figure 6). During the test period of the present study a small variation, around 2 Ω·m in the measurements was observed (corresponding to a coefficient of variation, CoV, at about 10%). Considering the CoV, the results obtained by two measurement techniques provide comparable results.

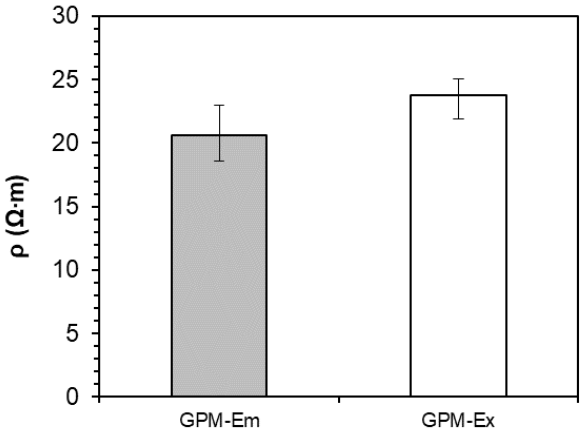

Figure 5. Electrical resistivity determined using the pre-embedded probe (GPM-Em) and the external plates (GPM-Ex). Specimens with constant mass in water bath (mean values and range of results variation).

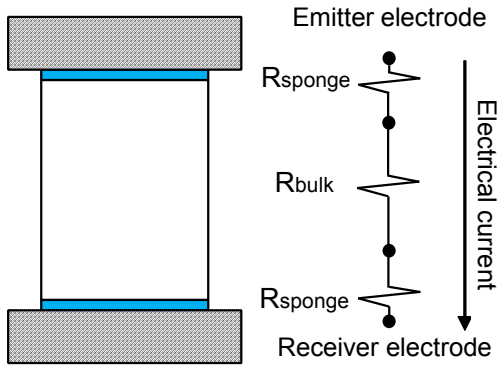

Figure 6. Simplified equivalent electric circuit between the emitter electrode and the receiver electrode when using the external plates (AC was used, i.e., the emitter and receiver electrodes are continuously switching place).

3.2 Effect of contact material on the evaluation of the electrical resistivity of the bulk material

Figure 7 shows the mean values and range of results variation of the electrical resistivity measured before (Figure 7a) and after (Figure 7b) carbonation of the grouts on all the specimens. Low and comparable resistivities, of about 20 Ω·m, were observed for the two different grouts in alkaline condition (GFA-Em and GPM-Em) (see Figure 7a). The carbonation of the grouts caused an increase in their resistivity, especially the commercial grout (GPM). Specimen GPM-Em-C reached values higher than 500 Ω·m; specimen GFA-Em-C showed resistivity of about 120 Ω·m, which is closer to the resistivity of the carbonated mortar specimen (M-Ex, ~170 Ω·m).

The resistivity measured on the prismatic carbonated mortar specimens with the post-embedded probes (M-postEm-GPM and M-postEm-GFA), ranging from 87 Ω·m to 110 Ω·m, was about half of that measured with the external plates on the cubic carbonated mortar specimen (M-Ex), which was around 170 Ω·m. This difference is attributed to the presence of the alkaline grout used as contact material between the post-embedded probe and the mortar; the alkaline grout had resistivity of about 20 Ω·m, which is one order of magnitude lower than that of the mortar. Using a grout with a higher resistivity than the mortar, which is the case for the carbonated commercial grout (M-postEm-GPM-C), values higher than 300 Ω·m were measured. Whereas using a contact material with a resistivity close to that of the mortar, its influence on the measurements of the resistivity of the mortar became negligible. This was observed for the specimen with GFA as contact material (M-postEm-GFA-C) after carbonation of the grout for which an electrical resistivity around 167 Ω·m. Thus, the presence of the grout can greatly affect the measured electrical resistivity carried out with the post-embedded probe and this depend on the difference in resistivity between the grout and the bulk, and the geometry of the system.

Considering eq. 4, the mortar resistivity can be determined with the post-embedded probe by measuring the grout resistivity and knowing the cell constants. These constants can be determined by numerical simulation.

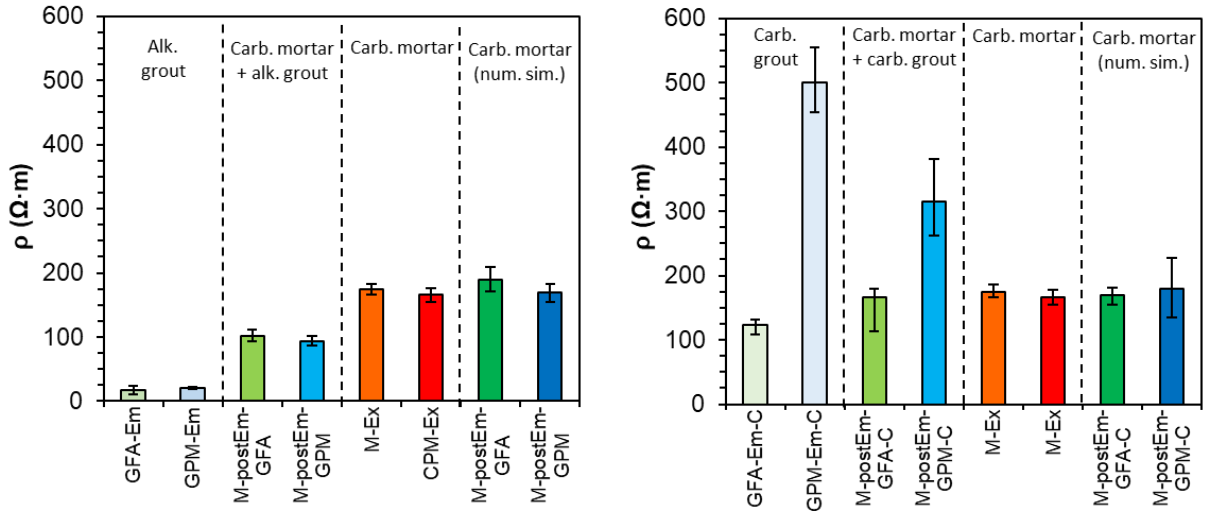

(a) (b)

Figure 7. Mean values (and range of results variation) of the electrical resistivity measured: (a) submerged, before accelerated carbonation; (b) submerged, after accelerated carbonation, and numerical results

3.3 Offset of contact material effect.

The offset of the effect of grout in the post-embedded probe was done by means of numerical iterations aimed at satisfying equation (6):

$$\rho_{system,\ measured} = (2*\rho_{grout}*k_{grout} + \rho_{mortar}*k_{mortar}) / k_{system} = \rho_{system,\ FEM} \quad (6)$$

where the $\rho_{system,\ FEM}$ is the electrical resistivity determined by the finite element model. The measured electrical resistivity of the grout (contact material) used as data input in the FEM and the electrical resistivity of the mortar determined by inverse analysis (Figure 4).

The average of the numerical results obtained by the iteration procedure described above is reported in Figure 7 (two sets of data on the right side of Figures 7a and 7b). The numerical results (M-postEm-GFA and M-postEm-GPM) of 170-190 Ω·m are close to the electrical resistivity of the mortar cubes (M-Ex) measured with the external plates (~170 Ω·m). The accuracy of the numerical simulations could be improved considering additional resistances that are in the electrical circuit such as the resistance at the interfacial zone between the grout and the mortar and the resistance at the interfacial zone between the electrode and the grout.

3.4 Effect of geometry of the system on the measurement

Further numerical simulations were performed to study the effect of some geometrical parameters on the predicted electrical resistivity when using post-embedded probes: The distance between the electrodes was varied from 50 mm to 10 mm and thickness of the grout of 1 mm, 2 mm and 3 mm were considered. An electrical resistivity of 10 Ω·m was assigned to the grout and 100 Ω·m to the mortar. The values represent alkaline and carbonated concrete, respectively, both with high moisture condition. The results of the simulations are reported in Figure 8. The figure illustrates how the setup, can influence the measurements. The calculated electrical resistivity of the system ($\rho_{system,FEM}$) decreases when decreasing the distance between the electrodes or increasing the thickness of the grout. Thus, the effect of the grout on the measure of the mortar resistivity with post-embedded probe can be reduced, besides the reduction of the difference between the resistivities of the two materials, by reduction of the thickness of the grout and increase in the distance between the electrodes.

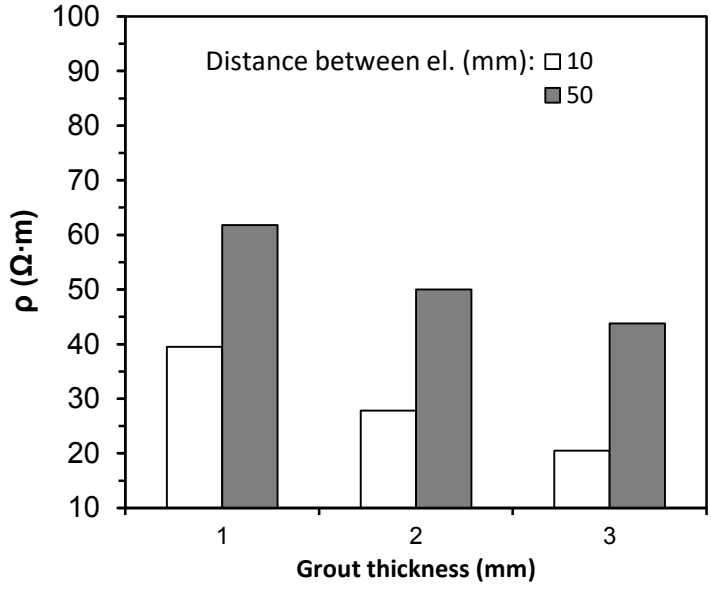

Figure 8. Numerical simulation results illustrating the impact on electrical resistivity of the system ($\rho_{system,\ FEM}$) of the distance between the electrodes and the thickness of the contact material (grout).

4. CONCLUSIONS

The experimental results showed that for the investigated material at capillary saturated condition, comparable electrical resistivity was measured with pre-embedded probe and external plates. This shows that the used of post-embedded sensors allows to monitor the electrical resistivity of cement-based materials over time, even when the grout carbonates.

When a post-embedded probe was used to determine the electrical resistivity, the measurement was affected by the resistivity of the contact material (grout) used for the installation and by the

geometry of the system (composed by the probe, the grout, and the cement-based material). The influence of the grout was negligible only if the resistivity of the grout was comparable to the resistivity of the bulk material. The effect of the grout on the measurement of bulk material resistivity with post-embedded probe can be reduced by reduction of the thickness of the grout and increasing the distance between the electrodes.

ACKNOWLEDGEMENTS

This work is part of the collaboration between Politecnico di Milano (POLIMI) and Norwegian University of Science and Technology (NTNU). The research was financed by the Italian Ministry of Education, University and Research (MIUR) for the project entitled “Predicting the service life of reinforced concrete structures by monitoring the electrical resistivity of concrete” and Lavkarbsem (NFR project no. 235211/O30) project, which is supported by the Norwegian Research Council and the following companies: Mapei AS, Norbetong AS, Norcem AS, Skanska AS, and Rambøll Engineering AS.

References

[1] W.J. McCarter, M. Emerson, H. Ezirim, Properties of concrete in the cover zone: developments in monitoring techniques, Magazine of Concrete Research 47 (1995) 243-251

[2] T.M. Chrisp, W.J. McCarter, G. Starrs, P.A.M. Basheer, J. Blewett, Depth-related variation in conductivity to study cover-zone concrete during wetting and drying, Cement and Concrete Composites 24 (2002) 415–426.

[3] C. Andrade, M. A. Sanjuán, A. Recuero, O. Río, Calculation of chloride diffusivity in concrete from migration experiments, in non steady-state conditions, Cement and Concrete Research 24 (1994) 1214-1228.

[4] R. B. Polder, W.H.A. Peelen, Characterisation of chloride transport and reinforcement corrosion in concrete under cyclic wetting and drying by electrical resistivity, Cement and Concrete Composites 24 (2002) 427–435.

[5] O. Sengul, Use of electrical resistivity as an indicator for durability, Construction and Building Materials 73 (2014) 434-441.

[6] C. Alonso, C. Andrade, J.A. González, Relation between resistivity and corrosion rate of reinforcements in carbonated mortar made with several cement types, Cement and Concrete Research 18 (1988) 687-698.

[7] G.K. Glass, C.L. Page, N.R. Short, Factors affecting the corrosion rate of steel in carbonated mortars, Corros. Sci. 32 (1991) 1283-1294.

[8] L. Bertolini, R.B. Polder, Concrete resistivity and reinforcement corrosion rate as a function of temperature and humidity of the environment, TNO Report 97-BT-R0574 (1994).

[9] K. Hornbostel, C.K. Larsen, M.R. Geiker, Relationship between concrete resistivity and corrosion rate–a literature review, Cement and Concrete Composites 39 (2013) 60-72.

[10] M. Messina, M. Gastaldi, L. Bertolini, Estimation of corrosion propagation in carbonated reinforced concrete structures by monitoring of the electrical resistivity of concrete, Metallurgia italiana 109 (2017) 51-54.

[11] C. Andrade, R. D'Andrea, A. Castillo, M. Castellote, The use of electrical resistivity as NDT method for the specification of the durability of reinforced concrete, Non Destructive testing in Civil Engineering – Nantes – France (2009).

[12] DuraCrete, Final technical report, Probabilistic performance based durability design of concrete structures, The European Union – Brite EuRam III (2000).

[13] R.N. Cox, R. Cigna, O. Vennesland, T. Valente (eds), Corrosion and protection of metals in contact with concrete, COST 509 (1997), Final report, European Commission, Directorate General Science, Research and Development, Brussels, EUR 17608 EN.

[14] H.W. Whittington, J. McCarter, M.C. Forde, The conduction of electricity through concrete, Magazine of Concrete Research 33 (1981) 48-60.

[15] L. Bertolini, B. Elsener, P. Pedeferri, R. Polder, Corrosion of steel in concrete, Wiley-VCH Verlag GmbH & Co. (2013).

[16] K. De Weerdt, G. Plusquellec, A. Belda Revert, M.R. Geiker, B. Lothenbach, Effect of carbonation on the pore solution of mortar, Cement and Concrete Research 118, (2019).

[17] W. Elkey, E.J. Sellevold, Electrical resistivity of concrete, Publication no. 80, Directorate of Public Roads Norway.

[18] M. Castellote, C. Andrade, M.C. Alonso, Standardization, to a reference of 25°C, of electrical resistivity for mortars and concretes in saturated or isolated conditions.

[19] R. Polder, C. Andrade, B. Elsener, Ø. Vennesland, J. Gulikers, R. Weidert, M. Raupach, Test methods for on site measurement of resistivity of concrete, Materials and Structures 33 (2000) 603-611.

[20] K. Reichling, M. Raupach, J. Broomfield, J. Gulikers, V. L'Hostis, S. Kessler, K. Osterminski, I. Pepenar, U. Schneck, G. Sergi, G. Taché, Full surface inspection methods regarding reinforcement corrosion of concrete structures, Materials and Corrosion 64 (2013) 116-127.

[21] Hooton, R.D., M.R. Geiker, and E.C. Bentz, Effects of Curing on Chloride Ingress and Implications on Service Life. ACI materials journal, 2002. 99: p. 201-206.

[22] F. Hunkeler, Monitoring of repaired reinforced concrete structures by means of resistivity measurements, Materials Science Forum 247 (1997) 93-106.

[23] M. Raupach, J. Gulikers, K. Reichling, Condition survey with embedded sensors regarding reinforcement corrosion, Materials and Corrosion 64 (2013) 141-146.

[24] H. Borsje, W.H.A. Peelen, F.J. Postema, J.D. Bakker, Monitoring alkali-silica reaction in structures, Heron special issue on ASR-ISSN 0046-7316 47 (2002) 156-165.

[25] W.J. McCarter, H.M. Taha, B. Suryanto, G. Starrs, Two-point concrete resistivity measurements: interfacial phenomena at the electrode – concrete contact zone, Measurement science and technology 26 (2015) 1-13.